Electronic structures and optical spectra of thin anatase TiO$_2$ nanowires through hybrid density functional and quasiparticle calculations

Hatice Ünal,[1] Oğuz Gülseren,[2] Şinasi Ellialtıoğlu,[3] and Ersen Mete[1, *]

[1]*Department of Physics, Balıkesir University, Balıkesir 10145, Turkey*
[2]*Department of Physics, Bilkent University, Ankara 06800, Turkey*
[3]*Basic Sciences, TED University, Ankara 06420, Turkey*
(Dated: March 25, 2014)

The electronic properties of quasi-one-dimensional anatase TiO$_2$ nanostructures, in the form of thin nanowires having (101) and (001) facets, have been systematically investigated using the standard, hybrid density functional and quasiparticle calculations. Their visible photoabsorption characteristics have also been studied at these levels of theories. The thin stoichiometric nanowire models are predicted to have larger band gaps relative to their bulk values. The band gap related features appear to be better described with the screened Coulomb hybrid density functional method compared to the standard exchange–correlation schemes. Depending on the self-consistency in the perturbative GW methods, even larger energy corrections have been obtained for the band gaps of both (101) and (001) titanium dioxide nanowires.

I. INTRODUCTION

Demand on efficient utilization of solar energy has drawn increasing attention to reducible metal oxides. The wide-gap semiconductor TiO$_2$ has gained utter importance in photovoltaics and photocatalysis due to its catalytically active and reducible surfaces, long standing stability, vast availability, and nontoxicity.[1] Under UV irradiation TiO$_2$ achieves hydrogen production from water since the position of the conduction band (CB) well aligns with the formation energy of hydrogen.[2] In addition to these properties, TiO$_2$ also has excellent charge carrier conduction features making it one of the best choices as the anode electrode in dye sensitized solar cells (DSSC).[3,4] Great effort has been made to extend its UV limited photoresponse to visible region by various adsorptional, substitutional or interstitial impurities.[5–8] Along with modification of the electronic structures, in this way, the already rich photocatalytic properties of titania can be further enhanced.[9–11]

Among the three polymorphs of TiO$_2$, the anatase phase shows the highest photocatalytic activity especially with (001) and (101) surfaces.[12–15] Although the rutile phase with (110) bulk termination forms a relatively more stable surface[16], anatase has been reported to be the most stable structure at nanodimensions.[17–20] Quasi-one-dimensional nanostructures have large surface-to-volume ratios. In particular, for the case of titania, this can be benefited in enhancement of efficiencies of photovoltaic and photocatalytic applications.

Nano-sized materials come into view with preferable and interesting physical and chemical properties.[21–23] For instance, quasi-one-dimensional periodic structures facilitate the transport of the charge carriers. Moreover, relaxation of surface strain during nanowire growth on a semiconductor substrate naturally avoids lattice mismatch problems observed in the thin film case.

This allows fabrication of defect-free materials.[24] Single-crystalline anatase TiO$_2$ nanowires were synthesized by Zhang *et al.* by using anodic oxidative hydrolysis and hydrothermal method.[25] Sol-gel coating,[26,27] and simple thermal deposition[28] methods were also successfully used to prepare highly crystalline anatase nanowires. Jankulovska *et al.* fabricated well-crystallized TiO$_2$ nanowires about 2 nm in diameter, using chemical bath deposition at low temperature.[29] Recently, Yuan *et al.* achieved a controlled synthesis of thin-walled anatase nanotube and nanowire arrays using template-basis hydrolysis.[30] Experimentally prepared thin nanowires show photoelectrochemical properties different from nanoparticulate TiO$_2$ electrodes. Especially, an increase in their band gap energies and photocatalytic oxidation powers was observed, which is attributed to the quantum-size effect.[29–32] Moreover, nanowire systems are capable of showing superior charge carrier transport features due to their one-dimensional nature.

The band gap-related properties of titania nanostructures have also been studied by several experiments.[29–33] Lee *et al.* used UV-vis spectra to demonstrate the band-gap modulation with particle size (ranging from 3 to 12 nm) in mesoporous TiO$_2$ nanomaterials.[32] Yuan *et al.* analyzed the tunability of the optical absorption edge of TiO$_2$ nanotubes and nanowires with respect to wall thickness and internal diameter.[30] Similar observations have been reported by Jankulovska *et al.* for very thin anatase nanowires.[29] Gloter *et al.* studied the energy bands of titania-based nanotubes with lateral size of ∼10 nm using electron energy-loss spectroscopy (EELS).[33]

On the theoretical side, Szieberth *et al.*, recently, investigated the atomic and electronic structure of lepidocrocite anatase nanotubes.[34] Fuertes *et al.* studied the absorption characteristics of nanostructured titania by using a self-consistent density functional tight-binding method.[20] Tafen and Lewis[35], and later on, Iacomino *et al.*[19] analyzed the effect of size and facet

structure on the electronic properties of anatase TiO_2 nanowires within the density functional theory (DFT) approach. The standard density functional exchange-correlation schemes tend to underestimate the fundamental band gap of titania by about 1 eV. Moreover, they fall short in describing defect related gap states.[11] Therefore, proper theoretical description of the electronic and optical structures of quasi-one-dimensional TiO_2 nanomaterials is necessary for a fundamental understanding in terms of pure science and for designing more efficient applications in terms of technology.

We employed standard and range separated screened Coulomb hybrid density functional methods and GW quasiparticle calculations to investigate the electronic properties, energy corrections and visible absorption profiles for thin stoichiometric anatase TiO_2 nanowire models having (101) and (001) facets. Our atomistic models represent the smallest possible diameter nanowires. Therefore, size effects might become apparent and can be discussed at different flavors of DFT based approaches considered in this work.

II. COMPUTATIONAL METHOD

We carried out total energy DFT computations using projector-augmented waves (PAW) method[36–38] to describe the ionic cores and valance electrons with an energy cutoff value of 400 eV for the plane wave expansion. Perdew–Burke–Ernzerhof (PBE) functional[39] based on the generalized gradient approximation (GGA) has been used to treat nonlocal exchange–correlation (XC) effects as implemented in the Vienna ab-initio simulation package (VASP).[36] The Brillouin zone was sampled using $10\times2\times2$ mesh of $\mathbf{k}$-points.

Inherent shortcoming of the standard DFT due to the lack of proper self-energy cancellation between the Hartree and exchange terms as in Hartree–Fock theory, causes the well-known band gap underestimation. In particular, strongly correlated $3d$ electrons localized on Ti atoms are not properly described. One of the alternatives to compensate this localization deficiency appears to be the screened Coulomb hybrid density functional method, HSE[40–42], which partially incorporates exact Fock exchange and semilocal PBE exchange energies for the short range (SR) part as,

$$E_{\mathbf{x}}^{\mathrm{HSE}} = aE_{\mathbf{x}}^{\mathrm{HF,SR}}(\omega) + (1-a)E_{\mathbf{x}}^{\mathrm{PBE,SR}}(\omega) + E_{\mathbf{x}}^{\mathrm{PBE,LR}}(\omega) \quad (1)$$

where a is the mixing coefficient[43] and ω is the range separation parameter.[40–42] The long range (LR) part of exchange and full correlation energies are defined by standard PBE[39] functional.

For the description of excitation processes in an interacting many particle system, Green's function theory is one of the appropriate methods through computation of the quasiparticle energies.[44,45] The quasiparticle (QP) concept makes it possible to describe the system through

a set of equations,

$$(T + V_{e\text{-}n} + V_{\mathrm{H}} - E_{i\mathbf{k}})\psi_{i\mathbf{k}}(\mathbf{r}) + \int \Sigma(\mathbf{r},\mathbf{r}',E_{i\mathbf{k}})\psi_{i\mathbf{k}}(\mathbf{r}')d\mathbf{r}' = 0 \quad (2)$$

where T is the kinetic energy operator, $V_{e\text{-}n}$ represents the electron–ion interactions, V_{H} is the Hartree potential, $E_{i\mathbf{k}}$ are the quasiparticle energies labeled by state number i and wave vector $\mathbf{k}$. The self-energy operator Σ accounts for the exchange and correlation effects and is given by

$$\Sigma(\mathbf{r},\mathbf{r}',\omega) = \frac{i}{2\pi}\int_{-\infty}^{\infty} e^{i\omega'\delta} G(\mathbf{r},\mathbf{r}',\omega+\omega')W(\mathbf{r},\mathbf{r}',\omega')d\omega' \quad (3)$$

where G is the Green's function representing the propagation of a hole or an additional particle in the presence of an interacting many particle system, and W is the dynamically screened Coulomb interaction. The QP energies can be determined iteratively by

$$E_{i\mathbf{k}}^{N+1} = E_{i\mathbf{k}}^{N} + Z_{i\mathbf{k}}\mathrm{Re}\big[\langle\psi_{i\mathbf{k}}|T + V_{e\text{-}n} + V_{\mathrm{H}} + \Sigma(E_{i\mathbf{k}})|\psi_{i\mathbf{k}}\rangle\big] \quad (4)$$

where $Z_{i\mathbf{k}}$ is the normalization factor.[46] We used PBE energy eigenvalues as the starting point and set $E_{i\mathbf{k}}^{1} = E_{i\mathbf{k}}^{\mathrm{PBE}}$ in Eq. (4) to get single shot $\mathrm{G}_0\mathrm{W}_0$[47,48] energy corrections up to the first-order perturbation theory. In the GW_0 case, the propagator in Eq. (3) is updated after the first iteration while screened Coulomb term, W, remains fixed.

Shishkin et al.[46] proposed a self-consistent GW (scGW) approach by recasting single-electron theory into the generalized eigenvalue problem after linearization around some reference energy $E_{i\mathbf{k}}^{N}$:

$$\overbrace{[T + V_{e\text{-}n} + V_{\mathrm{H}} + \Sigma(E_{i\mathbf{k}}^{N}) + \xi(E_{i\mathbf{k}}^{N})E_{i\mathbf{k}}^{N}]}^{\mathrm{H}(E_{i\mathbf{k}}^{N})}|\psi_{i\mathbf{k}}\rangle = \underbrace{E(1 - \xi(E_{i\mathbf{k}}^{N}))}_{\mathrm{S}(E_{i\mathbf{k}}^{N})}|\psi_{i\mathbf{k}}\rangle \quad (5)$$

where H is the non-Hermitian Hamiltonian, S is the overlap operator, and $\xi(E_{i\mathbf{k}}^{N}) = \frac{\partial\Sigma(E_{i\mathbf{k}}^{N})}{\partial E_{i\mathbf{k}}^{N}}$. Then, this can be mapped to a simple diagonalization problem, using the Hermitian parts of H and S matrices, H and S, in the DFT basis $\{\phi_i^N\}$,

$$S^{-1/2}HS^{-1/2}U = U\Lambda \quad (6)$$

where U is a unitary matrix and Λ is the diagonal eigenvalue matrix.[46] The wave functions are iteratively updated by $\phi_i^{N+1} = \sum_i U_{ij}\phi_i^N$ and the corresponding energies are $E_i^{N+1} = \Lambda_{ii}$. This approximation to the non-Hermitian problem in Eq. (5) results in $\sim 1\%$ deviation in band gaps.

Electron–hole interactions can be described by Bethe–Salpeter equation (BSE) for the two particle Green's function. In linear-response time-dependent density functional theory (TDDFT), the many-body effects
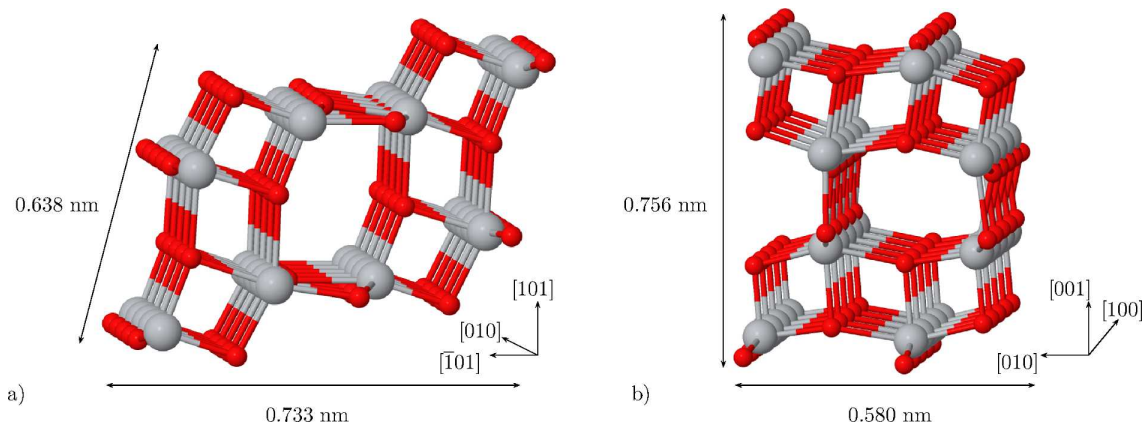
FIG. 1: Relaxed atomistic structures of the anatase (101) and (001)-nanowire models.

are contained in the frequency dependent exchange–correlation kernel, $f_{xc}(\mathbf{r}_1, \mathbf{r}_2; \omega)$. Reining[49] *et al.* derived a TDDFT XC-kernel from BSE to reproduce excitonic effects. Adragna *et al.*[50] and Bruneval *et al.*[51] suggested a similar approach to calculate the polarizability of a many-body system within the GW framework,

$$\chi = [1 - \chi_0(v + f_{xc})]^{-1}\chi_0 \qquad (7)$$

where χ_0 is the independent QP polarizability and v is the bare Coulomb kernel. We have included electron–hole interactions in our scGW calculations using Eq. (7) as implemented in VASP.[46]

The absorption spectra can be obtained by considering the transitions from occupied to unoccupied states within the first Brillouin zone. The imaginary part of the dielectric function $\varepsilon_2(\omega)$ is given by the summation,

$$\varepsilon_{\alpha\beta}^{(2)}(\omega) = \frac{4\pi^2 e^2}{\Omega} \lim_{q \to 0} \frac{1}{q^2} \sum_{c,v,\mathbf{k}} 2w_{\mathbf{k}}\delta(\epsilon_{c\mathbf{k}} - \epsilon_{v\mathbf{k}} - \omega)$$
$$\times \langle u_{c\mathbf{k}+\mathbf{e}_\alpha q}|u_{v\mathbf{k}}\rangle\langle u_{c\mathbf{k}+\mathbf{e}_\beta q}|u_{v\mathbf{k}}\rangle^* \quad (8)$$

where the indices c and v indicate empty and filled states respectively, $u_{c\mathbf{k}}$ are the cell periodic part of the orbitals and $w_{\mathbf{k}}$ are the weight factors at each $\mathbf{k}$-point.[52]

III. RESULTS & DISCUSSION

The minimum-energy band gap of bulk anatase TiO_2 with the standard PBE XC functional is found to be 2.03 eV indirect between Γ and a point close to X while the direct gap at Γ is 2.35 eV. These are inconsistent with the experimental results $(3.2 - 3.4$ eV).[53,54] The local density approximation (LDA/GGA) tends to distribute charge based on the properties of an homogeneous electron gas. In the case of TiO_2, this leads to an unsatisfactory description of localized $3d$ states of Ti. A Hubbard U term can be added only for the d-space in order to supplement repulsive correlation effects between the d-electrons. We performed a simple PBE+U calculation with U = 5 and get a band gap of 2.56 eV for the bulk anatase. Larger values of U increase this value but distort the lattice structure unacceptably. The range-separated hybrid DFT approach has a potential to improve energy gap related properties by incorporating HF exchange interaction. We previously found an indirect gap value of 3.20 eV using the HSE method with a mixing factor of $a = 0.22$.[55] Another alternative is to use perturbation theory to get quasiparticle energy shifts. In recent studies on TiO_2, Chiodo *et al.*[56], Landmann *et al.*[57] and Kang *et al.*[58] calculated the indirect electronic gap as 3.83 eV, 3.73 eV and 3.56 eV, respectively, at the single shot G_0W_0 level. Noticeable disagreement with the experiments is due to the choice of the starting point from the inaccurate DFT description of Ti $3d$ states. Patrick *et al.*[59] reported a gap of 3.3 eV by performing G_0W_0 calculation starting from DFT+U band structure while single shot GW on top of DFT wave functions gave a value of 3.7 eV. This approach still depends on the empirical U parameter even though it is computationally less demanding. For a parameter-free theory, one needs a self-consistent GW procedure. But self-consistency solely can not give desired accuracy without including electron–hole interactions. For this reason, we performed scGW calculations including vertex corrections[50,51] and calculated an electronic gap of 3.30 eV for the bulk anatase in good agreement with the experiments.[53,54]

For the quasi-two-dimensional cases, the optical spectra of the anatase surface is essentially similar to the absorption and photoluminescence (PL) data of the bulk.[60] Giorgi *et al.*[60] identified the first direct exciton at ∼3.2 eV on the anatase (001)-(1×1) surface from the QP calculations. At the nanoscale, the reduction of material sizes below the exciton radius gives rise to an increase of the band gap as a quantum confinement effect. The exciton radii for titania were estimated in between 0.75 nm and 1.9 nm.[61,62] The blue shift of the band gap becomes dominant for materials with cross section sizes fitting in this range.
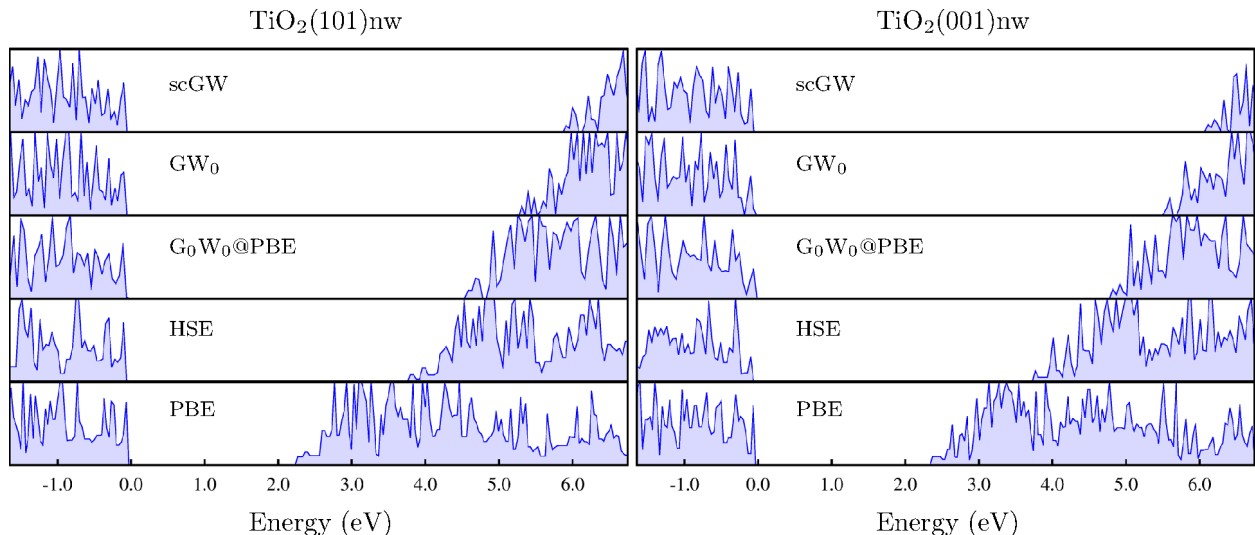
FIG. 2: Densities of states (DOS) plots of bare anatase (101)-nanowire and (001)-nanowire calculated using PBE, HSE functionals within DFT and G_0W_0, GW_0, scGW methods within many-body perturbation theory (MBPT) starting from PBE initial wavefunctions. The origin of the energy axis is set at just above the VBM.

In order to discuss the electronic structure and possible size effect at different level of density functional theories, thin nanowire models were built from the anatase form of TiO_2 having (001) and (101) facets. They will be referred as nw(001) and nw(101), respectively. We preserved the stoichiometry in building atomistic models, and did not saturate any of the dangling bonds exposed on the facets. Nanowire structures have been represented in a tetragonal supercell geometry using periodic boundary conditions, PBC. While the PBC along the nanowire axis leads to infinitely long wire, to prevent interaction between adjacent isolated wires, a large spacing of at least 20 Å perpendicular to the axis has been introduced. Initial geometries have been fully optimized based on the minimization of the Hellman–Feynmann forces on each of the atoms to be less than 0.01 eV/Å. The relaxed atomistic structures of the anatase nw(101) and nw(001) models as shown in Fig. 1 do not show any major reconstruction from their initial configurations cleaved from bulk structures. The Ti–O bond lengths on the facets get slightly larger than the bulk value of 1.95 Å. This deviation is much less inside the nanowire maintaining the anatase form for these isolated free-standing 1D thin nanostructures. Relaxation of surface atoms passivates possible surface states to appear in the band gap (see Fig 2).

TABLE I: Calculated band gaps (in eV) of TiO_2 nanowires

Nanowire	PBE	HSE06	G_0W_0@PBE	GW_0	scGW
(101)	2.51	4.01	4.88	5.60	6.05
(001)	2.69	4.06	5.15	5.79	6.25

For the TiO_2 nanotubes with internal diameters in the range $2.5 - 5$ nm, Bavykin et al.[63,64] estimated an optical gap of 3.87 eV from their absorption and PL studies. Yuan et al. reported a significant blue shift of the optical absorption edge as the wall thickness of anatase nanotubes decrease from 45 to 10 nm.[30] Similarly, the energy gap was reported to be 3.84 eV for 2D titanate nanosheets[65], and to be 3.75 eV for thin anatase TiO_2 films.[66] These are significantly larger than the bulk value of 3.2 eV.

We present the band gap values of thin anatase nw(101) and nw(001) structures calculated with various levels of theory in Table I. Although still underestimated, the standard PBE functional gives band gaps for these 1D systems larger than the bulk value of 2.03 eV. Admixing partial exact exchange energy through a screened Coulomb interaction, HSE method predicts the gaps as 4.01 eV and 4.06 eV for nw(101) and nw(001), respectively. Therefore, hybrid HSE functional largely improves over PBE results. Size effect for nw(001) and nw(101) having diameters ∼0.75 nm becomes remarkable at the hybrid DFT level. Even though hybrid DFT is not designed to describe absorption processes, the positions of lowest lying absorption peaks can reasonably be estimated by these methods.[11,55]

One of the methods to describe excitations is the time dependent density functional theory (TDDFT). Meng et al. used TDDFT method on a hydrogenated nanowire segment having anatase (101) facet as a finite system. Although, their nanowire segment is thicker than our model structures, the optical spectrum of the bare nanowire using TDDFT shows an increase in the band gap relative to the bulk value. Unexpectedly, Fuertes et al.[20] predicted an energy gap of 2.92 eV for an anatase cluster composed of 34 TiO_2 units using a time-dependent density functional tight-binding method. However, they mention possible involvement of surface states narrowing the gap.
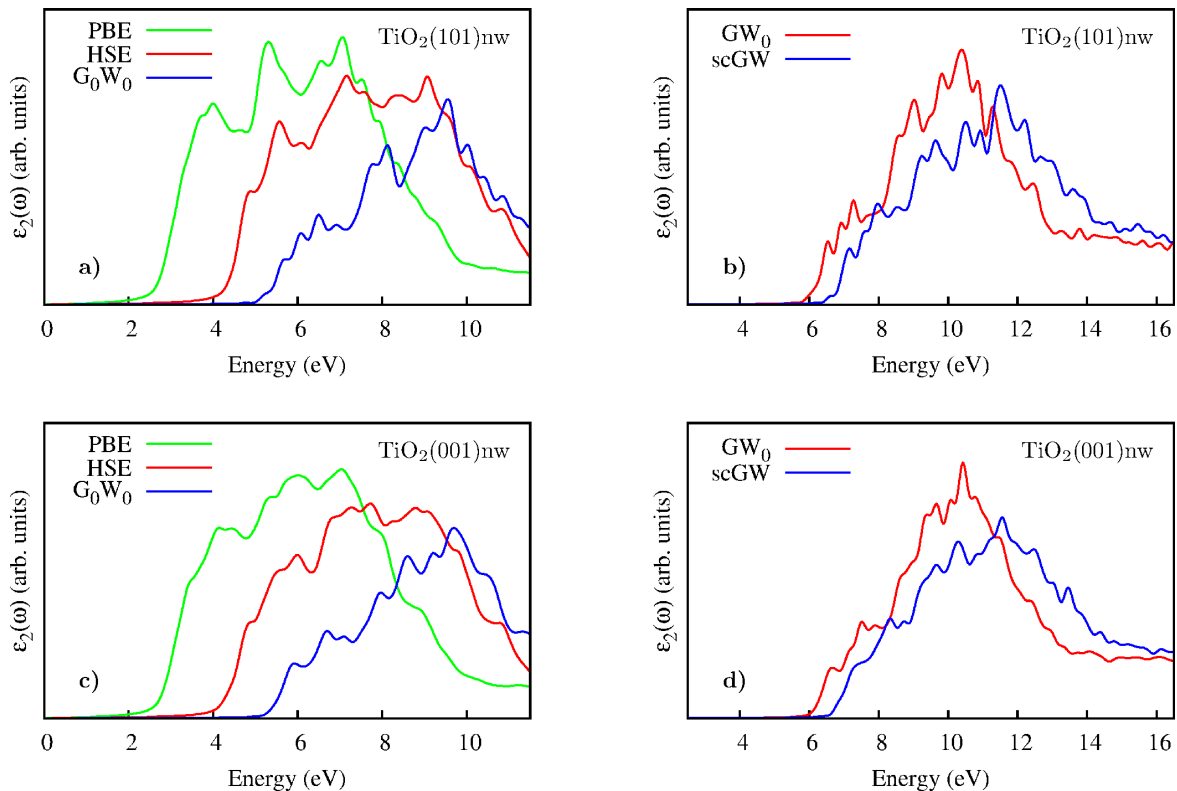
FIG. 3: Calculated absorption spectra for the anatase TiO_2 nw(101) and nw(001) nanowire models calculated with density functional PBE, HSE, G_0W_0, GW_0, and scGW methods.

Several experimental studies observed a blue shift of the optical gap as TiO_2 nanomaterial sizes decrease.[62,69–71] The liable quantum confinement effect is reported at different size regimes. For instance, Kumar et al.[71] reported a linear decrease in the energy gap from 3.83 eV to 3.70 eV with an increase in the fiber diameter from 60 nm to 150 nm. Anpo et al.[69] observed the size effect for particle sizes of several tens of nanometers while Serpone et al.[62] identified it for nanometer sized colloidal anatase particles. Lee et al.[32] estimated an inverse proportionality of the band gap to the nano particle size. For anatase, their prediction gets as large as 4 eV at a particle size of 2 nm.[32]

For a (0,n) lepidocrocite-type TiO_2 nanotube with a diameter of 1.81 nm, Szieberth et al. calculated a band gap of 5.64 eV using a density functional theory–tight binding (DFT-TB) method.[34] In a previous GW study, Mowbray et al. calculated the quasiparticle gap of a (4,4) TiO_2 nanotube having a diameter of 0.8 nm to be about 7 eV.[68] This QP gap value reflects an overestimation associated with the lack of self-consistency and excitonic effects in their GW calculations. Therefore, it was suggested as an upper bound for the optical gap. For the thin anatase (101) and (001) nanowires, ∼0.75 nm in diameter, our G_0W_0-predicted QP gaps are 4.88 eV and 5.15 eV, respectively. The blue shift of the gap is attributed to the quantum confinement effect which is strong in this size regime. In this sense, for the bare nanowires, our QP results can be considered more reliable relative to hybrid DFT methods where a portion of the exact exchange is mixed with the PBE exchange.

Along with the calculated energy gaps, similar conclusions can be drawn from the density of states, DOS, presented in Fig. 2. The valance band (VB) edge showing O 2p character slightly changes depending on the XC functional used or on the level of quasiparticle calculation performed. On the other hand, the conduction band (CB) edge which is mainly formed from Ti 3d states shifts and sets the value of the electronic band gap.

In GW_0 calculations, the self-consistency is imposed on the single particle propagator giving rise to larger energy corrections relative to those of G_0W_0. So, the QP gaps become to 5.60 eV for nw(101) and 5.79 eV for nw(001). The self-consistency in both the single particle propagator and the dynamical screening tends to shift the unoccupied Ti 3d states up to much higher energies. In our scGW calculations including electron–hole interactions, we obtained the QP gaps as 6.05 eV and 6.25 eV for the thin (101) and (001) nanowires, respectively. A trend of increasing energy correction with increasing level of theory is seen. A direct comparison of QP or hybrid DFT results with the experimental data is generally not straightforward due to possible involvement of stress, impurity or defect related states. Even so, our scGW calculations estimate the QP gaps in good agreement with previous experimental[32] and theoretical[34,68] findings.

For the discussion of the absorption spectra, the imaginary part of the dielectric function for anatase (101) and (001) nanowires are depicted in Fig. 3. For both of the nanowires, in all cases, the absorption starts around the conduction band edge energies consistent with the calculated band gaps. The VB maximum is dominantly populated with O $2p$ electrons. The CB minimum is characterized by Ti $3d$ t_{2g}-states. Hence, one can conclude that the first peak mainly contributed by the transitions from the states at the VB top to the states at the CB edge. Therefore, these transitions are dipole-allowed and are suitable for photocatalytic applications. The scGW-calculated optical spectra shows that the photo-response of defect-free anatase TiO_2 nanowires significantly blue shift up in the UV region for nanowire radii within the quantum confinement regime. In other words, as we employed more accurate density functional based theories starting from the standard PBE up to scGW including excitonic effects, we have obtained a trend of increasing blue shifts in the band gaps of anatase nanowires with diameters around 1 nm. Experimental observation of such a large quantum size effect might be concealed by possible presence of stress, impurity or defect related gap states.

IV. CONCLUSIONS

In summary, the electronic band gap and absorption properties of thin TiO_2 nanowires having (101) and (001) facets have been investigated at the levels of exact exchange mixed hybrid DFT and quasiparticle calculations with various self-consistency schemes. When the periodicity is reduced to one dimension as in the nanowire model structures, the small diameters result in larger electronic band gaps. Therefore, the dimensionality of the nano materials plays a critical role in the photoresponse of titania. Moreover, dye adsorbates or transition metal dopants will be crucially important to functionalize these semiconductor metal oxides under visible light illumination at the nano-scale. Such impurities also greatly influence efficiencies for photovoltaic and photocatalytic applications.

Range separated hybrid functionals incorporating exact exchange with $1/r$ Coulomb tail improve the electronic description of TiO_2 nanowires. Although they are not intended to get the excited state properties, photo absorption characteristics are also healed relative to traditional semi-local exchange-correlation schemes due partly to the shift of unoccupied states to higher energies. In order to get proper description of excited state properties one has to include electronic screening effects. This can be achieved by non-empirically range separated hybrid approaches or many body perturbative methods to calculate self-energy contributions. Higher levels of density functional theory increases accuracy at a computational cost. Consequently, a practical and reliable determination of size dependence of excitation gaps in TiO_2 nanomaterials are still desirable.

[*] Electronic address: emete@balikesir.edu.tr; Corresponding author

[1] U. Diebold, Surf. Sci. Rep. **48**, 53 (2003).

[2] A. Fujishima and K. Honda, Nature (London) **238**, 37 (1972).

[3] B. O'Regan and M. Grätzel, Nature (London) **353**, 737 (1991).

[4] A. Hangfeldt and M. Grätzel, Chem. Rev. **95**, 49 (1995).

[5] M. Grätzel, Nature (London) **414**, 338 (2001).

[6] S. Khan, J. M. Al-Shahry, and W. B. Ingler, Science **297**, 2243 (2002).

[7] M. Chen, Y. Cai, Z. Yan, and D. W. Goodman, J. Am. Chem. Soc. **128**, 6341 (2006).

[8] A. Fujishima, X. T. Zhang, and D. A. Tryk, Surf. Sci. Rep. **63**, 515 (2008).

[9] W. G. Zhu, X. F. Qiu, V. Iancu, X. Q. Chen, H. Pan, W. Wang, N. M. Dimitrijevic, T. Rajh, H. M. Meyer, M. P. Paranthaman, G. M. Stocks, H. H. Weitering, B. H. Gu, G. Eres, and Z. Y. Zhang, Phys. Rev. Lett. **103**, 226401 (2009).

[10] W.-J. Yin, H. Tang, Su-H. Wei, M. M. Al-Jassim, J. Turner, and Y. Yan, Phys Rev B **82**, 045106 (2010).

[11] V. Çelik, H. Ünal, E. Mete, and Ş. Ellialtıoğlu, Phys. Rev. B **82**, 205113 (2010).

[12] R. Hengerer, B. Bolliger, M. Erbudak, and M. Grätzel, Surf. Sci. **460**, 162–169 (2000).

[13] M. Lazzeri, A. Vittadini, and A. Selloni, Phys. Rev. B **63**, 155409 (2001).

[14] A. G. Thomas, W. R. Flavell, A. R. Kumarasinghe, A. K. Mallick, D. Tsoutsou, and G. C. Smith, Phys. Rev. B **67**, 035110 (2003).

[15] A. Selloni, Nat. Mater. **7**, 613 (2008).

[16] V. E. Heinrich and P. A. Cox, *The Surface Science of Metal Oxides*, (Cambridge Univ. Press, Cambridge, 1994).

[17] P. K. Naicker, P. T. Cummings, H. Zhang, and J. F. Banfield, J. Phys. Chem. B **109**, 15243–15249 (2005).

[18] J. E. Boercker, E. Enache-Pommer, and E. S. Aydil, Nanotechnology **19**, 095604 (2008).

[19] A. Iacomino, G. Cantele, F. Trani, and D. Ninno, J. Phys. Chem. C **114**, 12389–12400 (2010).

[20] V. C. Fuertes, C. F. A. Negre, M. B. Oviedo, F. P. Bonafé, F. Y. Oliva, and C. G. Sánchez, J. Phys.: Condens. Matter

25, 115304 (2013).

[21] X. Chen and S. S. Mao, Chem. Rev. **107**, 2891-2959 (2007)

[22] D. Çakır and O. Gülseren, J. Phys.: Conden. Matter **24**, 305301 (2012).

[23] D. Çakır and O. Gülseren, Phys. Rev. B **80**, 125424 (2009).

[24] P. Yang, R. Yan, and M. Fardy, Nano Lett. **10**, 1529–1536 (2010).

[25] X. Y. Zhang, L. D. Zhang, W. Chen, G. W. Meng, M. J. Zheng, L. X. Zhao, and F. Philipp, Chem. Mater. **13**, 2511 (2001).

[26] R. A. Caruso, J. H. Schattka, and A. Grenier, Adv. Mater. **13**, 1577 (2001).

[27] Y. Lei, L. D. Zhang, G. W. Meng, G. H. Li, X. Y. Zhang, C. H. Liang, W. Chen, and S. Z. Wang, Appl. Phys. Lett. **78**, 1125 (2001).

[28] B. Xiang, Y. Zhang, Z. Wang, X. H. Luo, Y. W. Zhu, H. Z. Zhang, and D. P. Yu, J. Phys. D **38**, 1152 (2005).

[29] M. Jankulovska, T. Berger, T. Lana-Villarreal, and R. Gómez, Electrochimica Acta **62** 172 (2012).

[30] L. Yuan, S. Meng, Y. Zhou, and Z. Yue, J. Mater. Chem. A **1**, 2552 (2013).

[31] T. Berger, T. Lana-Villarreal, D. Monllor-Satoca, and R. Gómez, J. Phys. Chem. C **112**, 15920 (2008).

[32] H.-S. Lee, C.-S. Woo, B.-K. Youn, S.-Y. Kim, S.-T. Oh, Y.-E. Sung, and H.-I. Lee, Top. Catal. **35**, 255 (2005).

[33] A. Gloter, C. Ewels, P. Umek, D. Arcon, and C. Colliex, Phys. Rev. B **80**, 035413 (2009).

[34] D. Szieberth, A. M. Ferrari, Y. Noel, and M. Ferrabone, Nanoscale **2**, 81 (2010).

[35] De Nyago Tafen and James P. Lewis, Phys. Rev. B **80**, 014104 (2009).

[36] G. Kresse and J. Hafner, Phys. Rev. B, **47**, 558 (1993).

[37] P. E. Blöchl, Phys. Rev. B **50**, 17953 (1994).

[38] G. Kresse and J. Joubert, Phys. Rev. B **59**, 1758 (1999).

[39] J. P. Perdew, K. Burke, and M. Ernzerhof, Phys. Rev. Lett. **77**, 3865 (1996).

[40] J. Heyd, G. E. Scuseria, and M. Ernzerhof, J. Chem. Phys. **118**, 8207 (2003).

[41] J. Heyd, G. E. Scuseria, and M. Ernzerhof, J. Chem. Phys. **124**, 219906 (2006).

[42] J. Paier, M. Marsman, K. Hummer, G. Kress, I. C. Gerber, and J. G. Angyan, J. Chem. Phys. **125**, 249901 (2006).

[43] J. P. Perdew, M. Ernzerhof, and K. Burke, J. Chem. Phys. **105**, 9982 (1996).

[44] L. D. Landau, JETP (USSR) **34**, 262; Soviet Phys. **7**, 183 (1958).

[45] V. M. Galitskii and A. B. Migdal, JETP **34**, 139; Soviet Phys. **7**, 96 (1958).

[46] M. Shishkin, M. Marsman, and G. Kresse, Phys. Rev. Lett. **99**, 246403 (2007).

[47] M. S. Hybertsen and S. G. Louie, Phys. Rev. B **34**, 5390–5413 (1986).

[48] R. W. Godby, M. Schlüter, and L. J. Sham, Phys. Rev. B **37**, 10159–10175 (1988).

[49] L. Reining, V. Olevano, A. Rubio, and G. Onida, Phys. Rev. Lett. **88**, 066404 (2002).

[50] G. Adragna, R. Del Sole, and A. Marini, Phys. Rev. B **68**, 165108 (2003).

[51] F. Bruneval, F. Sotille, V. Olevano, and L. Reining, Phys. Rev. Lett. **94**, 186402 (2005).

[52] M. Gajdoš, K. Hummer, G. Kresse, J. Furthmüller, and F. Bechstedt, Phys. Rev. B **73** 045112 (2006).

[53] H.Tang, F. Levy, H. Berger, and P. E. Schmid, Phys. Rev. B **52**, 7771 (1995).

[54] L. Kavan, M. Grätzel, S. E. Gilbert, C. Klemenz, and H. J. Schee, J. Am. Chem. Soc. **118**, 6716 (1996).

[55] V. Çelik, and E. Mete, Phys. Rev. B **86**, 205112 (2012).

[56] L. Chiodo, J. M. Garcia-Lastra, A. Iacomino, S. Ossicini, J. Zhao, H. Petek, and A. Rubio, Phys. Rev. B **82**, 045207 (2010).

[57] M. Landmann, E. Rauls, and W. G. Schmidt, J. Phys.: Condens. Matter **24**, 195593 (2012).

[58] W. Kang and M. S. Hybertsen, Phys. Rv. B **82**, 085203 (2010).

[59] C. E. Patrick, and F. Giustino, J. Phys.: Condens. Matter **24**, 202201 (2012).

[60] G. Giorgi, M. Palummo, L. Chiodo, and K. Yamashita, Phys. Rev. B **84**, 073404 (2011).

[61] C. Kormann, D. W. Bahnemann, and M. R. Hoffmann, J. Phys. Chem. **92**, 5196 (1988).

[62] N. Serpone, D. Lawless, and R. Khairutdinov, J. Phys. Chem. **99**, 16646 (1995).

[63] D. V. Bavykin, S. N. Gordeev, A. V. Moskalenko, A. A. Lapkin, and F. C. Walsh, J. Phys. Chem. B **109**, 8565 (2005).

[64] D. V. Bavykin, J. M. Friedrich, and F. C. Walsh, Adv. Mater. **18**, 2807–2824 (2006).

[65] N. Sakai, Y. Ebina, K. Takada, and T. Sasaki, J. Am. Chem. Soc. **126**, 5851 (2004).

[66] Y. R. Park and K. J. Kim, Thin Solid Films **484**, 34 (2005).

[67] S. Meng, J. Ren, and E. Kaxiras, Nano Lett. **8**, 3266 (2008).

[68] D. J. Mowbray, J. I. Martinez, J. M. Garc´a Lastra, K. S. Thygesen, and K. W. Jacobsen, J. Phys. Chem. C **113**, 12301–12308, (2009).

[69] M. Anpo, T. Shima, S. Kodama, and Y. Kubokawa, J. Phys. Chem. **91**, 4305 (1987).

[70] E. Joselevich and I. Willner, J. Phys. Chem. **98**, 7628 (1994).

[71] A. Kumar, R. Jose, K. Fujihara, J. Wang, and S. Ramakrishna, Chem. Mater. **19**, 6536 (2007).